SPRAY PROPERTIES OF ALTERNATIVE FUELS: A COMPARATIVE ANALYSIS OF MINERAL AND 1ST- 2ND GENERATION BIODIESEL

L. Allocca (*), E. Mancaruso, A. Montanaro, L. Sequino, B. M. Vaglieco

Istituto Motori CNR
Via G. Marconi 8 – 80125 Napoli - Italy

ABSTRACT

The paper presents the influence of biodiesel fuels on the injection process and their impact on the air-fuel mixture preparation. The experimental investigation was carried out on the fuel spray of a multi-jet common rail injection system both under non evaporative and evaporative conditions. The characteristics of the investigated spray include the fuel delivery, the instantaneous flow rate and the jet visualization, both within an optical high pressure vessel at ambient temperature and in an optically accessible single cylinder diesel engine for the evaporative conditions. The tests have been performed by means of a Bosch second generation common rail solenoid-driven fuel injection system with a 7-holes nozzle, flow number 440 cc/30s @100bar, 148deg cone opening angle (minisac type). Double injection strategy (pilot+main) has been implemented on the ECUs corresponding to operative running conditions of the commercial EURO 5 diesel engine. First and second generation biodiesel, like Soybean Methyl Ester (SME) and Gas To Liquid (GTL), have been used and their behaviour has been compared to the reference diesel fuel.

The images of evolving fuel, acquired in non-evaporative conditions and in the combustion chamber of the optical diesel engine, have been processed extracting the main parameters of the jet evolution. Different spatial distributions of the liquid fuel in the chamber have been assessed by the analysis of the luminous intensity along the jet direction. Moreover a comparison of the tip penetration measured by means of the experimental data and Hiroyasu and Siebers theoretical correlation has been made and showing very good agreements in both the systems.

INTRODUCTION

The decrease of petroleum reservoirs and the increase of interest to environment pollution problems has request a better knowledge on alternative fuels for diesel engines too [1]. In particular, the biodiesel is technically competitive with conventional petroleum-derived diesel fuel and requires virtually no changes in the fuel distribution infrastructure. For this reason and its biodegradability, the use of biodiesel is considered a good alternative to fossil fuels [2]. Moreover, there is evidence that the biodiesel, fuelling the engine, can have a strong impact on performances and pollutant emissions. In particular, the last generation electronically controlled diesel engines using biodiesel have shown a decrease in the emission of particulate matter and unburned hydrocarbons [3]. The feedstock used for the biodiesels production interferes with the human food chain, and the production costs are very high. These are the two main problems of the first generation biodiesel. For this reason, researchers are making considerable efforts in the development of an alternative production path, leading to the so-called second generation of biodiesel. The 1st generation is essentially a blend of methyl-esters while the 2nd are paraffin hydrocarbons [4]. It seems that there is a potential to reduce gaseous and smoke emissions using biodiesel blends, when an engine and its auxiliary systems (fuel injection, EGR) have been optimized for the specific blend.

The injection process of biodiesels influences the atomization and dispersion of the fuel in the combustion chamber. Consequently, the combustion process and the exhaust emissions depend on the mixture preparation during the ignition delay. Many researchers reported the relationship between these processes and chemical characteristics of the fuel/biofuels or their blends studied in quiescent vessel optically accessible [5, 6]. Recently, Pastor et al. [7] have investigated by means optical diagnostics the evolution of liquid phase penetration of evaporating sprays under engine-like conditions, with pure Rapeseed Methyl Ester (RME) fuel and blends with 5% and 30% mass rate of RME with diesel fuel. Injection pressure ranged between 30 and 160 MPa for a real 8-hole nozzle. In-cylinder ambient conditions at a constant density of 25 kg/m^3 and two values of peak temperature (815 and 905 K) were considered, using pure Nitrogen as intake gas. Results have shown that liquid length was dependent on biodiesel blend rate, but it was not fully controlled by the less volatile RME fraction. Moreover, the use of pure RME or blended with diesel fuel did not change the effect of injection pressure on liquid spray penetration, and the influence of ambient temperature was quite similar to that obtained from other wide range studies for diesel fuel.

Ochoterena et al. [8] applied optical diagnostics in order to analyze the spray development and combustion of oxygenated (RME) and Fischer-Tropsch fuels (GTL). The studies were carried out in the high-pressure, high-temperature spray test rig under conditions similar to those prevailing in a direct-injected diesel engine prior to injection. Results pertaining to spray behaviour showed that high-viscosity fuels had wider spray cone angles, smaller discharge coefficients (C_d) and shorter vapour penetration than low-viscosity fuels. The continuous liquid phase penetration was related to differences in surface tension, viscosity and density while the penetration of droplets and ligaments was related to volatility. Their

(*) corresponding author: l.allocca@im.cnr.it – tel +39 081 7177152 – fax +39 081 2396097

penetration was short for highly volatile fuels and long for low-volatility fuels. However, these researches have been carried out in system simulating engine-like condition and did not consider the chemical activity of the pilot injection/combustion characteristic of new high pressure Common Rail injection systems.

The research activity described in this paper is a study that involves fuel injection both in spray bomb investigations and in single-cylinder engine in order to assess the various biodiesel types on combustion behaviour including performance, specific fuel consumption, GHG (Greenhouse Gas and pollutant emissions). Optical diagnostics based on imaging have been applied both in high-pressure optically accessible quiescent vessel for non-evaporating investigation and in the combustion chamber of a DI diesel engine for evaporating/combustion conditions using two pure biofuels, Soybean Methyl Ester (SME) and Gas To Liquid (GTL). The injection rates have been measured for all the used fuel and the defined injection strategies. The fuel penetration, spray atomization, air/fuel mixing and cone angle have been analyzed in non evaporating and evaporating conditions for multi injection strategies performed with last generation Common Rail (CR) high pressure injection system. It is typical of new generation Euro 5 diesel engines.

EXPERIMENTAL SETUPS AND PROCEDURES

The effects on the injection process of the physical and chemical properties of a commercial diesel and two alternative diesel fuels are the main objective of the present study. The injection process characterization has been carried out under non evaporative conditions injecting the fuel within stagnant inert gas in a high-pressure optically-accessible cylindrical vessel in order to measure the spatial and temporal distribution of the fuel. Moreover, the injection process has been studied in an optically accessible single cylinder Common Rail diesel engine representing evaporative conditions similar to the real engine. The selected engine working conditions have been extracted from the ECU map of a commercial EURO 5 engine. They are 1500 rpm at 0.2 MPa of break mean effective pressure (BMEP) and 2000 rpm at 0.5 MPa of BMEP, respectively. The corresponding injection pressures are 50 and 73 MPa.

Feature	Method	Diesel	GTL	SME
Density @ 15 °C [kg/m3]	EN ISO 12185	840.1	777.5	884.4
Viscosity a 40 °C [mm2/s]	EN ISO 3104	3.141	2.547	3.958
Oxydation stability [g/m3]	EN ISO 12205	0.1	0.8	1.2
Lubricity a 60 °C [micron]	EN ISO 12156-1	-	235	174
Cetane Number	EN ISO 5165	51.8	73.9	48
Net Heat Value [MJ/kg]	ASTM D3338	43.1	43.53	37.25

Table 1 –Physical properties of mineral fuel and first and second generation biofuels.

The implemented injection strategy consists of pilot + main pulses and has been fixed for all fuels. A Bosch second-generation common rail system has been used to inject the fuel through a CRI2.2 injector with 7-hole nozzle, 440 cc/30s @10 MPa flow number, 148 deg cone opening angle (minisac type). First generation of biodiesel, Soybean Methyl Ether (SME), and second one, Gas To Liquid (GTL), have been used and their behaviours have been compared to the reference diesel fuel. A comparison of physical properties of the mineral diesel fuel, the first and second generation of biodiesels is reported in Table 1.

Non-evaporative experimental setup

The experimental activity has implied the measurement of instantaneous fuel injection rates on suitable test rig and the spatial-temporal evolution of the jets sprayed from the nozzle in a spray bomb. A sketch of experimental apparatus and further details on the analysis procedure has been reported in [9].

A Programmable Electronic Control Unit (PECU) controlled the injection apparatus, thus enabling to set the strategies in terms of pulse number and timing. Fast electronic drivers in the PECU has allowed setting precise and stable injections like the one involving small fuel quantities in multiple injections. The high pressure pump supplying the fuel to the CR has been driven by a variable speed electric motor while a heat exchange system on the hydraulic circuit has been adopted to keep a constant fuel temperature in the tank, (21±1 °C).

The fuel injection rate has been measured by an AVL Fuel Injection Gauge Rate System fitted on the Bosch tube inlet. The whole injected fuel per stroke is the integral of the instantaneous fuel rate over the total injection time [10]. The amount of injected fuel obtained has been successfully compared with the one pounded at the Bosch tube discharge by a precision balance.

The spatial and temporal evolution of the injected fuel have been measured by digital processing of the spray images detected at different time from the start of injection in an optically-accessible quiescent vessel filled at engine-like gas densities. SF_6 gas (density=6.2 kg/m^3) has been used in the vessel at room temperature reaching the desired gas densities at lower pressures than air. Pressures of 0.28 and 0.36 MPa have been set in order to achieve engine-like gas density of 17.5 and 22.6 kg/m^3, respectively. The images of evolving jets have been detected by a VCO - CCD camera (1376x1040 pixels, 12 bit, 0.5 μs shutter time) synchronized both with the injection system and the start of a set of high intensity flashes. The camera has been equipped with two lens groups (F/1:2.8): a 95 mm macro with a resolution of 18.8 pixels/mm for the analysis of the pilot injection and a 50 mm lens with a resolution of 10.1 pixels/mm (for the main pulse). These configurations have allowed the acquisition of images with a field of view capable to cover the complete evolution of the sprays.

Several images of consecutive injections have been acquired at each time-step. The stability and uniformity of the evolving sprays has made these conditions confident with a statistical evaluation on the spread of the parameters under study.

The analysis of the liquid fuel spray images has been carried out by Image ProPlus software that allows the image acquisition, the background subtraction and filtering, the edges determination, the tip penetration and cone angle measures.

Optical Engine

In order to study the spatial and temporal evolution of the fuel jets in an evaporative system a transparent diesel engine has been used. The transparent single-cylinder engine has been equipped with head and Common Rail injection system of the four-cylinder, 16 valves, 1.9l, standard production engine. In particular, the engine had the stroke of 92 mm, and the bore of 85 mm. To compensate the slightly lower compression ratio, typical of the optical engines, and to match the in-cylinder conditions of the real multi-cylinder engine, an external air compressor has been used. It supplied pressurized in-take air. The air has been filtered, dehumidified, and preheated. Moreover, a cooled EGR system has been used and a pressure valve has been set in the exhaust pipe in order to ensure the correct operation of the burned gas recirculation system. Moreover, the engine has been equipped with the variable swirl actuator (VSA) systems in order to manage the air swirl motion in the intake manifold. Finally, the engine has been equipped with the same common rail injection system used in non evaporative conditions, and the injector has been controlled by a fully flexible Electronic Control Unit (ECU) for combustion optimization.

A 46 mm diameter flat window has been fitted in the piston to provide a full view of the combustion bowl locating an appropriate 45° UV-visible fixed mirror inside the extended piston. The window has been realized with UV-grade fused silica. Digital imaging analysis has been performed by a CCD camera. The CCD camera with 640 x 480 pixels had a high sensitivity over a wide visible range and it was equipped with a 55 mm objective F/1:3.5 (10.4 pixels/mm). Two external highly luminous CW halogen lamps have been used to light the spray. Images at 1500 rpm have been acquired with an exposure time of 55 μs while images at 2000 rpm have been acquired with an exposure time of 41 μs. More details and specifications about the engine specifications and the optical set-up are reported in ref. [11].

IMAGE PROCESSING TECHNIQUE

An alternative method for the analysis of the jet has been developed in order to distinguish different density portion inside the jet shape. From a general point of view when a jet has been lighted, the denser zone reflects higher intensity of light than the low dense one. Analysing the spray images from both the non-evaporative and evaporative system, a relationship between the image luminous intensity and the jet density has been found. This method uses matrix manipulation and image processing techniques. Softwares like Matlab® and ImageJ® have been used.

The images have been saved in 8 bit format, 256 gray scale intensities representing the several luminous levels. The jets shapes have been cut out so that the chamber brightness wouldn't affect the jets luminosity analysis. The images have been processed using the "imcontour" function of Matlab® that draws a contour plot of the intensity image [12]. The light intensity along the jet axis has been investigated in order to evaluate the spray density during the penetration in the combustion chamber. Matlab® function "improfile" has been used, in order to compute the intensity values along a line or a multiline path in the jet image.

RESULTS

In Table 2 the amount of injected fuel in the pilot pulse and the complete injection are reported for all the tested fuels operating. Due to SME lower energy content with respect to the mineral fuel, the main pulse duration has been increased for achieving equivalent power output. The instantaneous amount of discharged fuel has been derived from the injection pressure peak in the injector adapter on the AVL meter. The total quantity has been obtained by integrating the pressure signal over the injection duration.

		DIESEL		GTL		SME	
P_{inj} [MPa]	Inj. time [μs]	pilot [mg/str]	Q_{tot} [mg/str]	pilot [mg/str]	Q_{tot} [mg/str]	pilot [mg/str]	Q_{tot} [mg/str]
50	350_820_600	1.41	7.61	1.52	7.41	-	-
50	350_820_640	-	-	-	-	1.54	8.69
73	260_1120_560	1.05	11.99	0.98	11.55	-	-
73	260_1120_590	-	-	-	-	0.79	13.74

Table 2 – Pilot pulse and total injected fuel for the different fuels and engine conditions

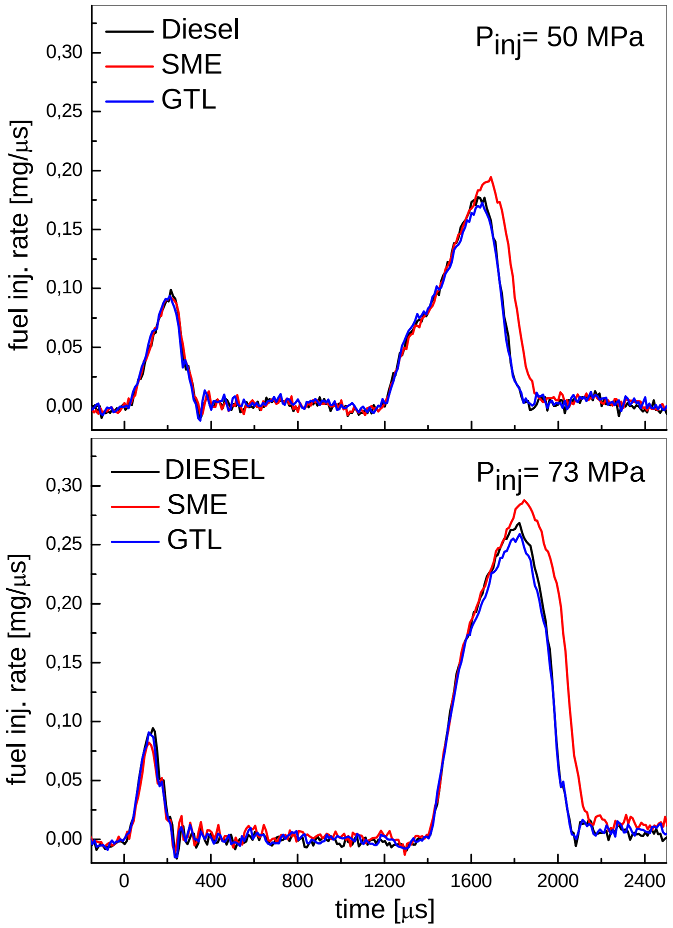

Figure 1 – Fuel injection rate profiles for the different investigated fuels and both operative conditions

Figure 1 reports the injection rate profiles for the three fuels and for both engine conditions. The profiles have a quite similar behaviour in terms of rise time and slope and no differences appear vs the different densities/viscosities of the fuels. The time scale has been chosen setting the initial point at the first fuel exit from the nozzle for the pilot pulse.

Consequently, the main injection appears around 1200 μs and 1400 μs after the start of the pilot for the low and high load condition respectively. Each profile is averaged on one hundred shots. The spray penetration of the liquid tip has been measured from the edges of the spray as described in the experimental apparatus and procedure paragraph. The spray penetration has been considered as the biggest distance of the fuel droplet from the nozzle [12]. Moreover, the 7 jets spray penetration is presented as the average of the 5 images repetitions at the same conditions in order to reduce the intrinsic irregularity of the spray evolution due to the non-uniform flow field within the chamber.

The single and averaged tip penetrations profiles versus time from the start injection have been analyzed for all fuels. They have initial linear trends with slight differences between sprays, indicating a good stability of the injection process. Figure 2 reports the main pulse tip penetration for each jet, labelled ‘1’-‘7’, in non evaporative system. The low load condition (P_{inj} =50 MPa) is shown at the left while the high load one (P_{inj} =73 MPa) is at the right. It is worthwhile to note that the anisotropy between the jets is negligible in both the investigated conditions and for the different fuels. Some differences in the jets penetration appear only at the lowest injection pressure and vessel gas density for Diesel and GTL main pulse. It is probably due to their lowest density and viscosity. At the highest load, the fuel penetration process is more stable and less dependent on chemical-physical properties of the fuels.

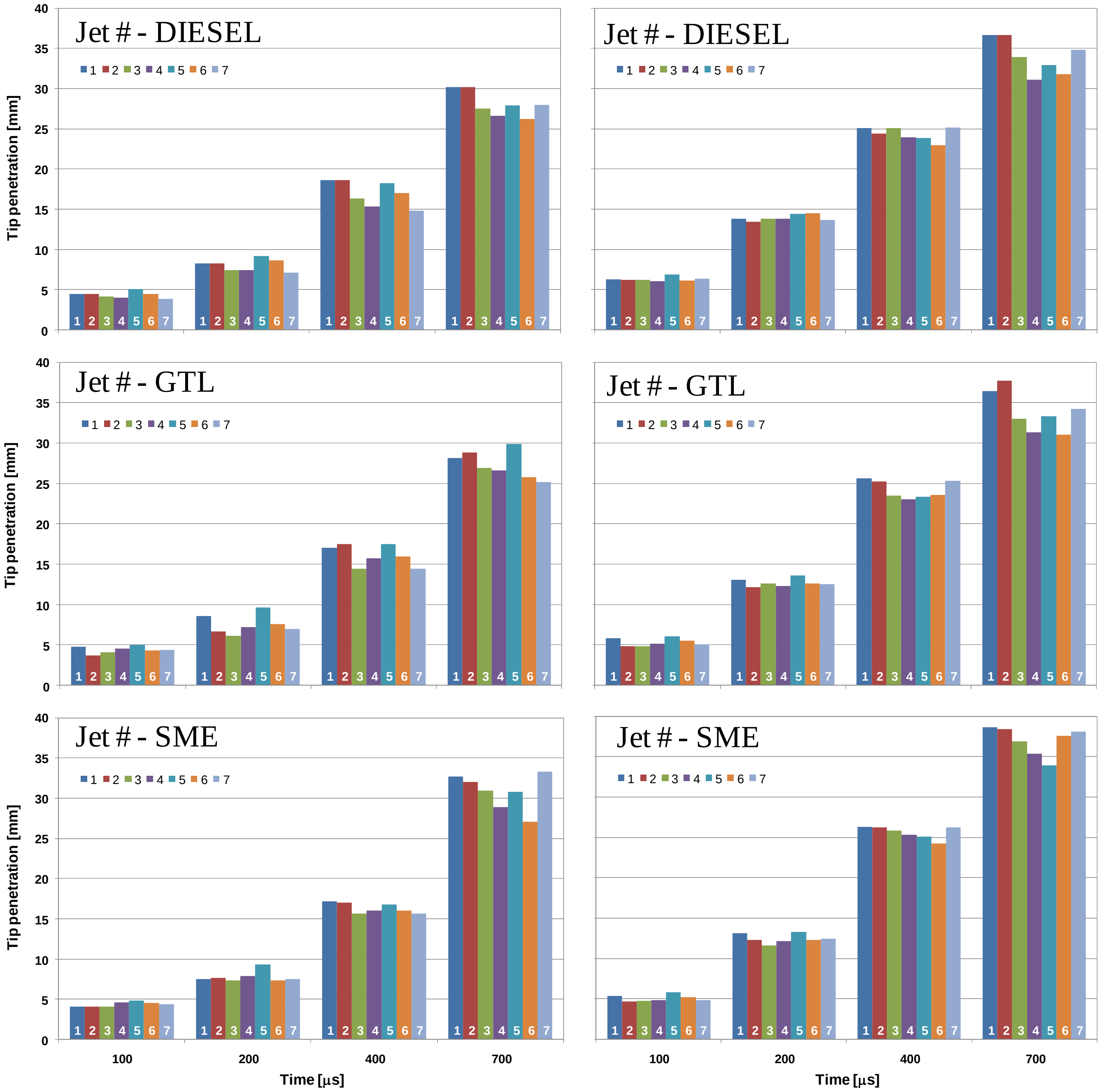

Figure 2 – Tip penetration for each jet of the main pulse in non evaporative system at the P_{inj} 50 MPa (left) and 73 MPa (right).

The comparisons of the tip penetration under evaporative and non evaporative conditions for the pilot and main injection, are reported in Figure 3 for both operative conditions. The curves relative at the injection pressure of 50 MPa (on the top) show a typical slope. They are split into two segments both for the pilot and the main pulses. In the first part, a good partly covering occurs for the spray penetrations for all the fuels except for the pilot of the Diesel fuel. The pilot penetrations are quite similar up to 200-250 µs while the mains overlap up to 500 µs. Later a less penetrating trend for the engine evaporative conditions is shown due to the vaporization process. At the injection pressure of 73 MPa (on the bottom) the effects of the vaporization process on the main penetrations are more evident. The penetration detachments became effective around 50 µs after the start of the injection (SOI).

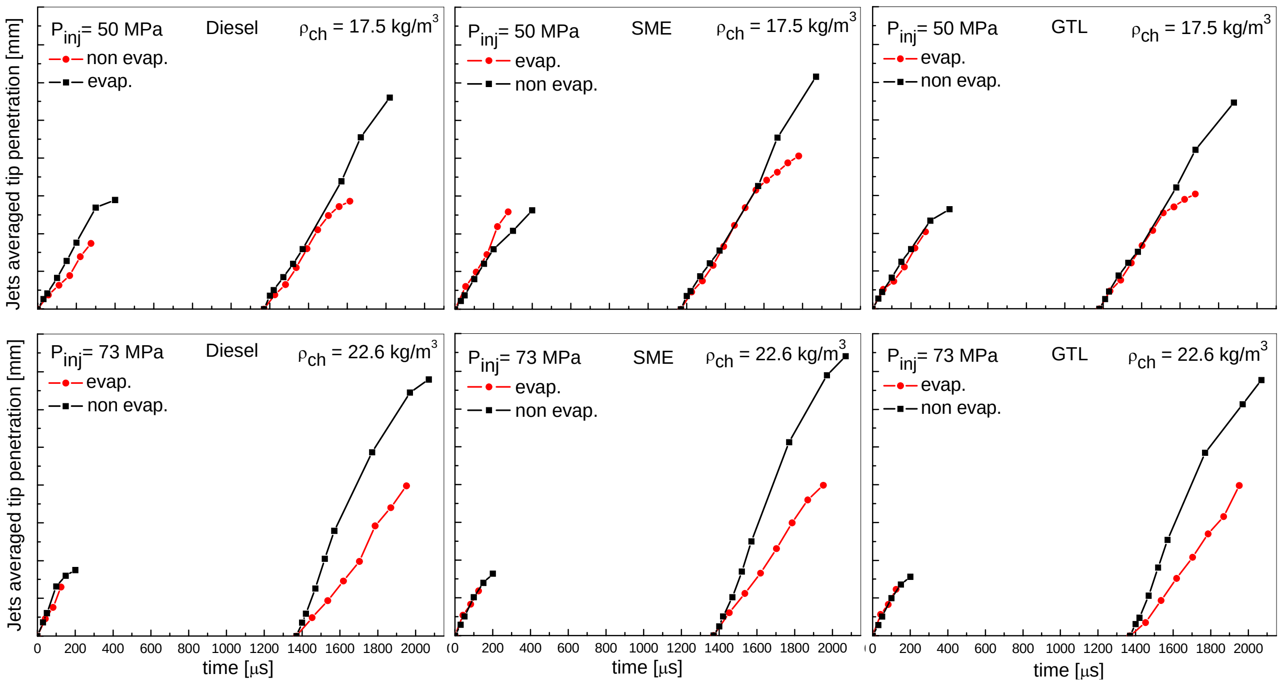

Figure 3 - Comparison of liquid jet penetration profiles under evaporative (optical engine) and non-evaporative conditions.

In order to better understand the liquid spatial distribution of the several fuels, the spray images detected in the combustion chamber and in non evaporative system have been processed using the procedure described in the Image Processing technique paragraph. A comparison has been evaluated between the images of the injection evolution that occur in the non evaporative system. In particular, the fuel rich zone reflects higher percentage of light with respect to less dense zone, it is possible to recognize the fuel liquid spatial distribution.

In Figure 4 are reported the liquid spatial distribution of the jets detected in the non evaporative system for both operative conditions at fixed time. The analysed images have been detected at 400 µs after the start of the main injection (ASOI). In the figure, the jets show a liquid core and a decreasing liquid density moving towards the jet boundaries. Jets at low load condition show a bigger dispersion and an indented and less distinct contour. Moreover, their luminosity values cross all the pixel intensity scale. While at high load condition, the SME fuel shows a denser liquid core with respect to the other

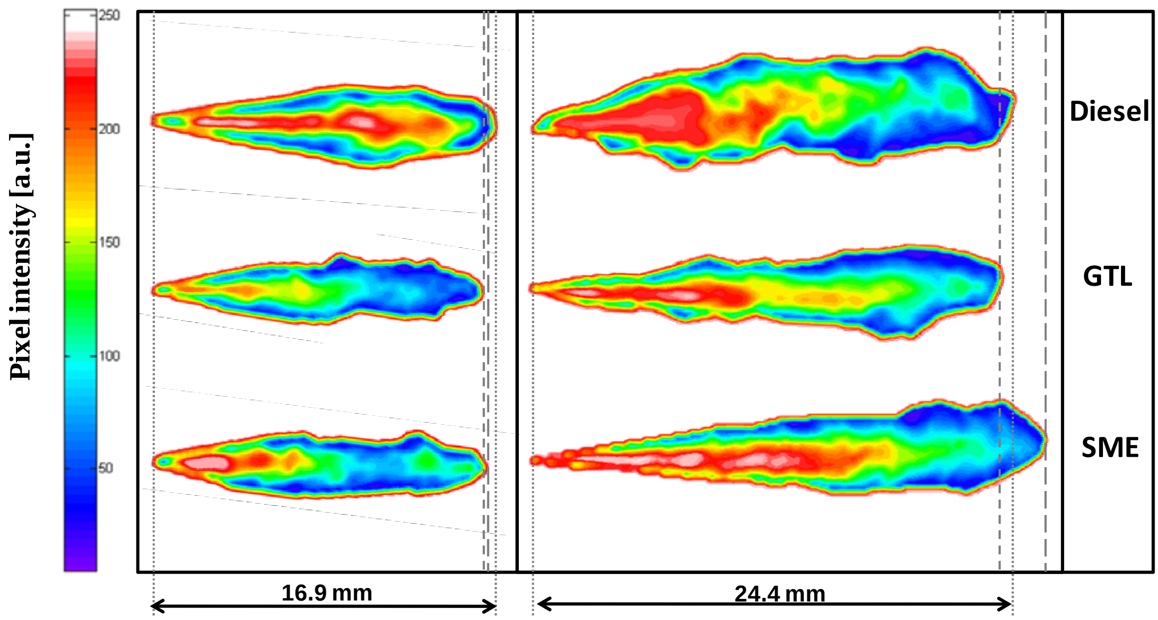

Figure 4 –Jet liquid densities for the investigated fuels in non evaporative system at 400µs after the SOI for the low load condition (Pinj =50MPa) and the high load condition (Pinj=73 MPa).

ones and a higher penetration because of the highest density/viscosity. These results fairly agree with previous data [13].

The average tip penetration curves under evaporative and non-evaporative conditions for the main injection have been compared with the Hiroyasu theoretical correlation (Figure 5) [14]. In order to summarize pure fuels behaviours, the tip penetration of Diesel and SME, respectively, are reported. Hiroyasu included two different phenomena influencing jet penetration. In the early instants, the injection pressure has the most important role in the process. Later, the effect of gas density in the cylinder becomes more significant and influences jets behaviour. Hiroyasu considered the breakup time (t_b) as the event that splits these two phenomena and computed it as reported below.

$$t_b = \frac{29 \rho_f d_n}{(\rho_g \Delta p)^{1/2}} \qquad (1)$$

$$t < t_b \qquad S = 0{,}39 \left(\frac{2\Delta p}{\rho_f} \right)^{\frac{1}{2}} t \qquad (2)$$

$$t > t_b \qquad S = 2{,}95 \left(\frac{\Delta p}{\rho_g} \right)^{0{,}25} (d_n t)^{\frac{1}{2}} \qquad (3)$$

Δp is the difference between the injection pressure and the pressure in the cylinder [Pa]; ρ_f, the fuel density [kg/m^3]; ρ_g, the density of the air into the cylinder [kg/m^3]; d_n the nozzle nominal diameter [n].

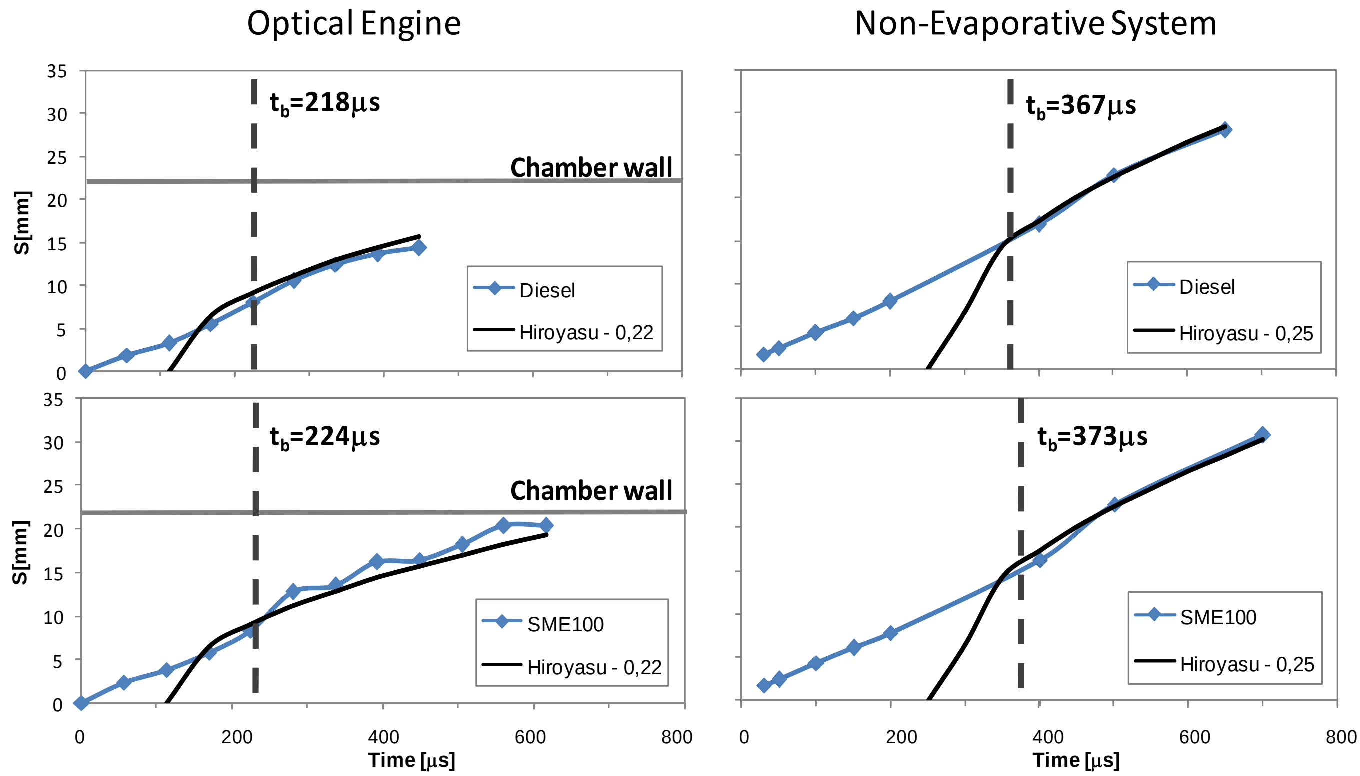

Figure 5 - Comparison between liquid jet penetration of main injection and Hiroyasu theoretical correlation under evaporative (left) and non-evaporative (right) conditions with P_{inj}=50 MPa for Diesel and SME fuels

In Figure 5, a good agreement between Hiroyasu correlation and average penetration curves for non-evaporative system is observed. On the contrary, in the optical engine, it has been necessary to modify the exponent of the term depending on pressure and gas density in equation 3. It allows to the data to fit with the model. On the other hand, Sibers et al. have modified this coefficient in a range of 0.25÷0.5 [15]. This is probably depended on the different enviroment an engine versus a bomb [16]. Finally, in order to fit the experimental data with the theoretical correlation it has been necessary to add a shift between the two curves. This is due to the slow penetration period that occurs in the early injection phase, when the injector needle reduces the orifice area for the passage of the fuel [17]. The dotted line represents the breakup time (t_b). It is proportional to the fuel density as observed in Table 1. Moreover, it occurs at different time after the start of main injection for Diesel and SME in the optical engine: 218 μs and 224 μs, respectively. On the other hand, in the non-evaporative system, it occurs at 367 μs and 373 μs after the start of main injection for Diesel and SME, respectively.

From a general point of view, in diesel engine equipped with high injection pressure system and injector with small nozzle diameter (as well as characterized by high in-cylinder density due to high boost) the fuel jet results in a complete atomization regime inside the spray very close the nozzle exit [13]. Under these conditions, the local transfer rates of momentum, mass and energy between liquid droplets and surrounding air are fast. Consequently, the transition time from the spray dominated by injected liquid to a spray controlled by entrained air is reduced in the optical engine with respect to the non-vaporized system. Finally, the fuel droplets evaporate as long as and there is enough air for them to heat up and vaporise. Moreover, vaporization is controlled by the fuel-air mixing rate within the spray.

In order to better understand the spray behaviour in evaporative and non-evaporative environment the results have been compared with theoretical correlation of Siebers. This correlation applied to high pressure common rail injection system and elaborated a new provisional model of jet penetration on the basis of the Hiroyasu's one. Siebers has realised a non-dimensional correlation between time (t*) and penetration (S*) [17]. The jet behaviour was considered still influenced by two phenomena: the liquid injected in the first phase and the air entrainment in the second. The transition between the two phases occurs when t*=1.

The Siebers' correlation is:

$$t^* = \frac{S^*}{2} + \frac{S^*}{4} \cdot \sqrt{1 + 16S^{*2}} + \frac{1}{16} \cdot ln\left(4S^* + \sqrt{1 + 16S^{*2}}\right)$$

It is characterised by two limits:

for short time: $\lim_{\tilde{t}\to 0} S^* = t^*$

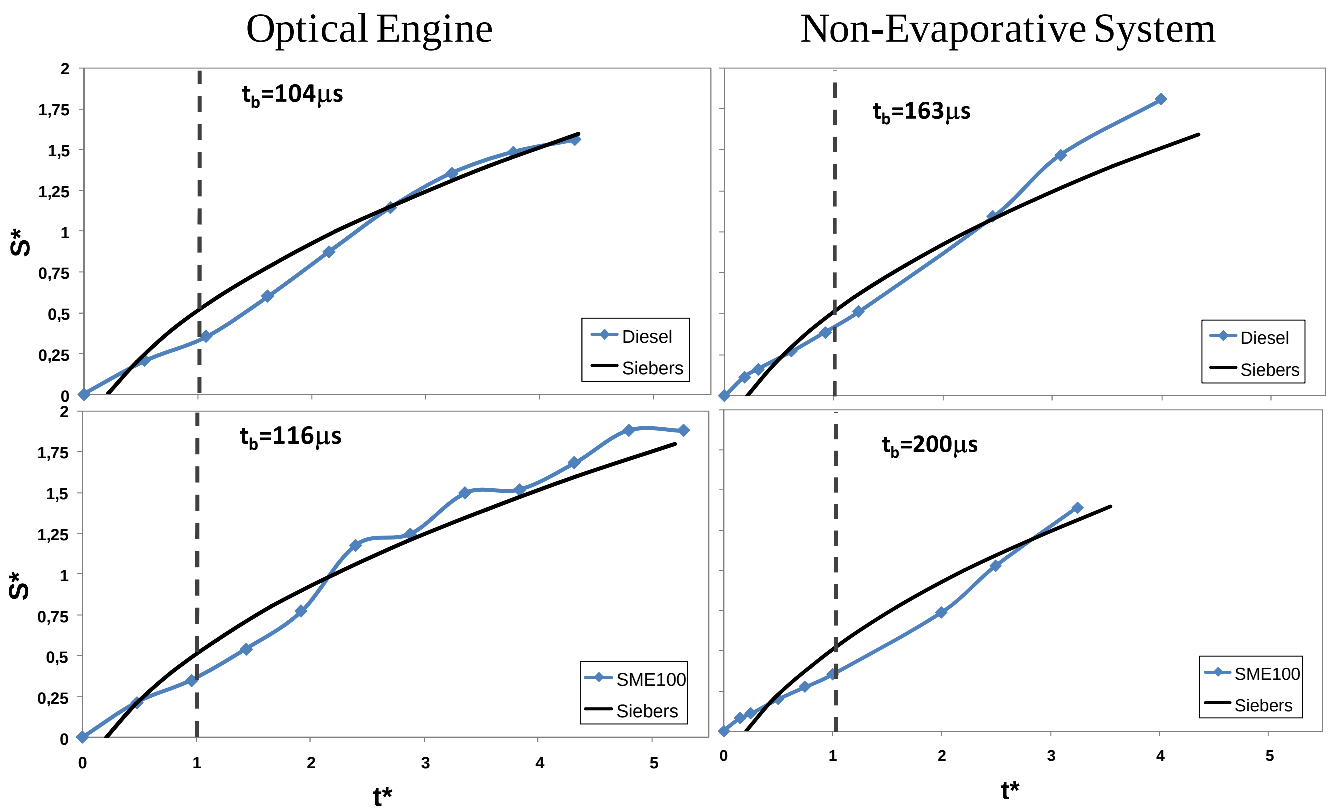

Figure. 6 - Comparison between liquid jet penetration of main injection and Siebers non-dimensional correlation under evaporative (left) and non-evaporative (right) conditions with P_{inj}=50 MPa for Diesel and SME fuels

for long time: $\lim_{\tilde{t}\to \infty} S^* = t^{*\,1/2}$

Finally, a small consideration can be made about the comparison of experimental data with Hiroyasu and Siebers' correlation. Hiroyasu's curve must be modified for the evaporative system and it needs an high value of shift for the non-evaporative one. On the contrary Siebers' correlation seems to fit well with the data in both systems without any correction and, moreover, it was necessary a smaller value of the shift.

The main difference between the two used models is probably due to the use of a high pressure common rail injection system by Siebers, while on the other hand Hiroyasu used a low pressure injection system.

In the first phase there is a linear dependence from time, for long time it follows the square root. More details are reported in [17].

In Figure 6 it can be noted a good agreement between the experimental data and the theoretical correlation for both environment and fuels. No modifications of the model have been necessary in this case, this is mainly due to the non-dimensional form that takes in account injector geometry, fuel properties and operating condition. Just a little shift has been used because, in the first instants of injection, the needle movement toward its seat influences the available flow area.

Some more observations regard the time of transition (t_b), it is still proportional to the fuel density and is longer for the non-evaporative system. Moreover the values obtained from Siebers' model correspond to almost half of the values calculated with the Hiroyasu's correlation.

CONCLUSIONS

In this paper it is reported a study on the effects of alternative diesel fuels on the air/fuel mixture process, both in non evaporative and evaporative engine-like conditions. Reference diesel fuel, first and second generation biodiesels, Soybean Methyl Ether and Gas-To-Liquid, respectively, have been injected by a common rail injection system through a 7-hole nozzle for Euro5 engine. Fuel injection rate measurements have been carried out for the different fuels, the spray evolution and the fuel dispersion/vaporization have been extracted by processing the images collected both in quiescent high-pressure vessel and single-cylinder engine for the determination of tip penetration curves and liquid spatial distribution of the jets. A comparison with Hiroyasu and Siebers theoretical correlations has been made.

The main results on the quiescent high-pressure vessel and single-cylinder engine have put into evidence the following:

- equivalent fuel quantity is delivered at equivalent injection conditions since it is negligible the effect of the fuel chemical characteristics;
- a good stability/uniformity of jet behaviour results from the statistical analysis of their parameters in the high-pressure/room-temperature conditions for all the investigated fuels and blends;
- the comparison of the spray penetrations in non evaporative and evaporative conditions shows an initial trend to overlap, while a shorter penetration in the evaporative environment seems, at longer time from the start of injection, due to the droplet evaporation;
- jets at low load condition show a bigger dispersion and an indented and less distinct contour while at high load condition, the SME fuel shows a denser liquid core with respect to the other ones and a higher penetration because of the highest density/viscosity
- the comparison of the spray penetrations in non-evaporative and evaporative conditions with Hiroyasu theoretical correlation shows a good agreement of the data, although these have been shifted in time in order to fit the curve. In the optical engine it has been necessary to modify the coefficient of the term depending on pressure and gas density. This is due to the different nature of the optical engine with respect to the non evaporative system;
- Siebers' correlation seems to fit well the data in both systems without any correction and it was necessary a smaller value of the shift.

ACKNOWLEDGMENTS

The authors wish to thank Mr. Carlo Rossi and Bruno Sgammato for maintaining the experimental apparatus and for their precious help.

NOMENCLATURE

- ASOI: After SOI
  GTL: Gas To Liquid
- ATDC: After TDC
  MLIP: Maximum Luminous Intensity Point
- BTDC: Before TDC
  RME: Rape Methyl Ester
- CA: Crank Angle
  TDC: Top Dead Center
- CR: Common Rail
  SME: Soybean Methyl Ester
- ECU: Electronic Control Unit
  SOI: Start Of Injection
- EGR: Exhaust Gas Recirculation
  VSA: Variable Swirl Actuator

REFERENCES

[1] Janaun, J., Ellis, N., "Perspectives on biodiesel as a sustainable fuel", Renewable and Sustainable Energy Reviews 14, pp.1312–1320, 2010

[2] Murugesan, A., Umarani, C., Subramanian, R., Nedunchezhian, N., "Bio-diesel as an alternative fuel for diesel engines-a review", Renew Sustainable Energy Rev 13 (3), pp. 653–662, 2009

[3] Lapuerta, M., Armas, O., Rodriguez-Fernandez, J., "Effect of biodiesel fuels on diesel engine emissions", Progress in Energy and Combustion Science 34, pp 198-223, 2008

[4] Allocca, L., Montanaro, A., Cipolla, G., Vassallo, A., "Spatial-Temporal Characterization of Alternative Fuel Sprays from a Second-Generation Common-Rail Fuel Injection System for Euro4 Passenger Car Application", SAE Paper 2009-01-1856, 2009

[5] He, C., Ge, Y. S., Tan, J., Han, X. K., "Spray Properties of Alternative Fuels: a Comparative Analysis of Biodiesel and Diesel", Int. J. Energy Res. 32, pp 1329-1338, 2008

[6] Gao, Y., Deng, J., Li, C., Dang, F., Liao, Z., Wu, Z., Li, L., "Experimental Study of the Spray Character-istics of Biodiesel Based on Inedible Oil", Biotechnology Advances 27, pp 616-624, 2009

[7] Pastor, J. V., Pastor, J. M., Gimeno, J., Nerva, J., (2009) The effect of Biodiesel fuel blend rate on the Liquid-phase fuel penetration in Diesel engine conditions. SAE Paper 2009-24-0051.

[8] Ochoterena, R., Larsson, M., Andersson, S., Denbratt, I., (2008) Optical studies of spray de-velopment and combustion characterization of oxygenated and Fischer–Tropsch fuels. SAE Paper 2008-01-1393.

[9] Alfuso, S., Allocca, L., Caputo, G., Corcione, F. E., Montanaro, A., Valentino, G., "Experimental Investi-gation of a Spray from a Multi-jet Common Rail Injection System for Small Engines", SAE Paper 2005-24-090, 2005

[10] Allocca, L., Alfuso, S., Corcione, F. E., "Assessment of Dynamic Performances of Diesel Solenoid Injec-tors for a Multiple Injection Common Rail System", SAE Paper 2003-01-21, 2003

[11] Mancaruso, E., Merola, S. S., Vaglieco, B. M., (2008) Study of the multi-injection combustion process in a transparent direct injection common rail diesel engine by means of optical techniques. In-ternational Journal of Engine Research, Vol 9 - No 6, pp 483-498.

[12] Kim, H. J., Park, S. H., Lee, C. S., (2010) A study on the macroscopic spray behaviour and atomization characteristics of biodiesel and dimethyl ether sprays under increased ambient pressure. Fuel Processing Technology 91, pp 354–363.

[13] Allocca, L., Mancaruso, E, Montanaro, A., Vaglieco, B. M., "Alternative Diesel Fuels Characterization in Non-Evaporating and Evaporating Conditions for Diesel Engines", SAE Paper 2010-01-1516

[14] Hiroyasu, H. and Arai, M., (1980) Fuel Spray Penetration and Spray Angle in Diesel Engines. Trans. JSME, 44-385, 3208-3220.

[15] Naber, J. D., Siebers, D. L., (1996) Effects of Gas Density and Vaporization on Penetration and Dispersion of Diesel Sprays., SAE Paper 960030.

[16] Hay, N., Jones, J. L., (1972) Comparison of the Various Correlations for Spray Penetration. SAE Paper 720076.

[17] Dennie L. Siebers, "Effects of gas density and vaporization on penetration and dispersion of diesel sprays", SAE 960034, 1996.